

PROCESSES OF HYDRODYNAMICS AND HEAT  
EXCHANGE IN DESCENDING BUBBLE FLOWS

B. G. Ganchev and V. G. Peresad'ko

UDC 532.529.5:536.242

The gas content, hydraulic resistance, heat transfer, and structure of descending bubble flows are investigated in the regimes of concurrent flow and of hovering of the gas phase.

The processes of hydrodynamics and heat exchange were studied in three vertical cylindrical channels, the heights and inside diameters of which were 2.5 m and 40 mm; 19 m and 52 mm; 3 m and 27 mm, respectively. The liquid (water) and the gas (air) were introduced into the channel in its upper part through a mixing device of the ejector type; in the first channel the liquid was supplied by a central jet while the air was supplied through an annular peripheral channel; in the second and third channels the liquid was introduced through an annular nozzle with a major diameter equal to the inside diameter of the channel, and was supplied in the form of a film on the channel wall, while the air was supplied through a central nozzle. The first channel was made of plastic with transparent walls, the second of stainless steel with three 3-m transparent inserts, and the third of copper pipe with an external electrical heater on a section 1.6 m long. The hydrodynamics was studied in all three channels, while heat transfer was studied only in the third channel.

To determine the gas content averaged over a cross section we used three types of resistance sensors incorporated into bridge circuits: with two annular electrodes mounted flush on the channel wall with a distance between them equal to a diameter; laminated sensors made of three plane electrodes 2 mm wide and 0.5 mm thick with sharp edges, located in a diametral cross section of the channel; and sensors with a central electrode mounted on an insulating holder at the axis of the channel with electrically conducting walls, the second electrode being the channel wall. The relative error in determining the average gas content did not exceed 0.01.

The distribution of gas content over a channel radius was investigated by the perforation method using L-shaped resistance sensors, described in detail in [1], for example.

The volume of bubbles in the flow was determined by the method of continuous sampling [2]. To measure the velocity of the liquid phase we used Pitot tubes with a receiver head diameter of 1.6/1.0 mm. The temperature distribution over a cross section was studied with Chromel—Alumel thermocouples with an open bead 0.06 mm in diameter. The pressure variation over the channel height was recorded with liquid manometers. The maximum relative error in measuring the static pressure gradient is 0.05.

The investigation was made in the following ranges of variation of the main parameters: reduced liquid velocity  $u_{\text{r0}} = 0.08-1.6$  m/sec; flow-rate volumetric gas content  $\beta = 0-0.31$ ; true volumetric gas content in the channel  $\varphi = 0-0.55$ ; temperature of the mixture  $\theta = 4-65^\circ\text{C}$ ; absolute pressure in the channel  $p = 0.08-0.22$  MPa.

In descending flows the liquid velocity is opposite to the rise velocity of the bubbles. If the liquid velocity exceeds the rise velocity, a regime of concurrent flow occurs, when the directions of the resultant velocities of the gas and liquid coincide. But if the average liquid velocity equals the group velocity of rise of the gas bubbles, a regime of hovering of the gas phase develops, when the true gas content can vary within wide limits in the complete absence of gas consumption. The bubbles undergo fluctuations relative to a certain center of equilibrium, changing their shape in the process. In the character of the interaction of the phases this regime is the opposite of the widely investigated bubbling regime described in the literature. In our experiments the hovering regime developed, for example, when the liquid column was supplied to the channel in a film flowing down its walls with a constant

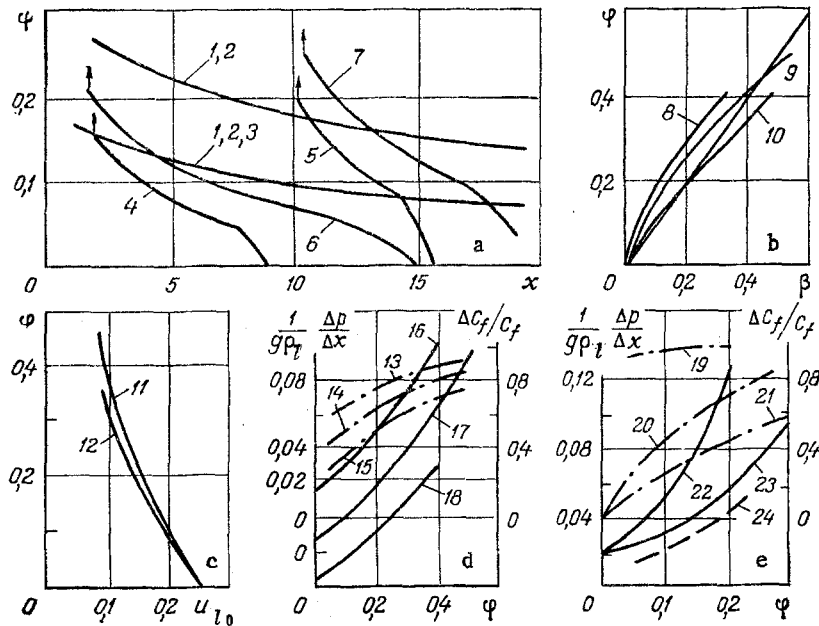


Fig. 1. Gas content and hydraulic resistance in descending bubble flows: a, e) peripheral entry of liquid,  $d = 52$  mm; b, d) central entry,  $d = 40$  mm,  $\theta = 5^\circ\text{C}$ ,  $p = 0.1$  MPa; 1-3, 8-10, 13-18, 20-23) concurrent flow; 4-7, 11, 12, 19, 24) hovering; 1-3)  $\theta = 20^\circ\text{C}$ ; 1)  $u_{l0} = 1$  m/sec; 2) 0.45 m/sec; 3) 0.29 m/sec; 4-7)  $u_{l0} = 0.204$  m/sec; 4, 5)  $\theta = 50^\circ\text{C}$ ; 6, 7)  $30^\circ\text{C}$ ; 8-10)  $5^\circ\text{C}$ ; 8, 13, 18)  $u_{l0} = 0.265$  m/sec; 9, 14, 17) 0.347 m/sec; 10, 15, 16) 0.575 m/sec; 11) central entry,  $d = 40$  mm,  $p = 0.1$  MPa; 12) peripheral entry,  $d = 27$  mm,  $p = 0.1$  MPa; 13-15)  $\Delta C_f/C_f$ ; 16-18)  $\Delta p_{fr}/\Delta x\rho g$ ; e)  $\theta = 20^\circ\text{C}$ ; 20-23)  $u_{l0} = 1$  m/sec; 20, 22)  $p = 0.22$  MPa; 21, 23) 0.12 MPa; 19-21)  $\Delta C_f/C_f$ ; 22-24)  $\Delta p_{fr}/\Delta x\rho g$ ; 19, 24)  $u_{l0} = 0.168$  m/sec;  $L = 4$  m.  $x$ , m.

pressure above the water level. A dynamic two-phase layer of one height or another develops in the upper part of the liquid column, depending on the position of the water level in the channel, the liquid flow rate, and the temperature. If the two-phase layer does not reach the exit from the channel, stable hovering of the gas phase is observed. But if it extends to the exit from the channel, gas circulation begins and concurrent flow develops — annular flow in the upper part of the channel above the water level and bubble flow below the level. Another way to obtain a bubble structure in the hovering regime is to shut off the gas supply to the channel and reduce the pressure above the water level. At a certain ratio of the pressures at the channel exit and above the water level the continuity of the liquid flow is disrupted, bubble flow is formed, the "excess" gas is washed out of the stream, and stable hovering of the gas phase develops. The integral characteristics (gas content and frictional losses) of descending bubble flows are shown in Fig. 1. The nonuniformity of the distribution of gas content over the channel height, in both the concurrent and the hovering flow, attracts attention first of all. The gas content decreases downstream in connection with the increase in pressure. And if the gas content in concurrent flow proves to be the same for two regimes in any one cross section, it also practically coincides over the entire channel height. There is a rather wide region of volumetric flow-rate gas content when  $\varphi > \beta$ .

The dependence of the true volumetric gas content on the flow-rate gas content in the regime of concurrent flow is approximated by the expressions

$$\varphi = \beta / [\beta + C(1 - \beta)]; \quad (1)$$

$$C = A\beta + B; \quad (2)$$

$$A = 2,818 \exp(-0,8865 Ar_\sigma 10^{-5}); \quad (3)$$

$$B = 0,52 Fr_\sigma^{0,213} \exp(-0,112 Ar_\sigma 10^{-5}) \quad (4)$$

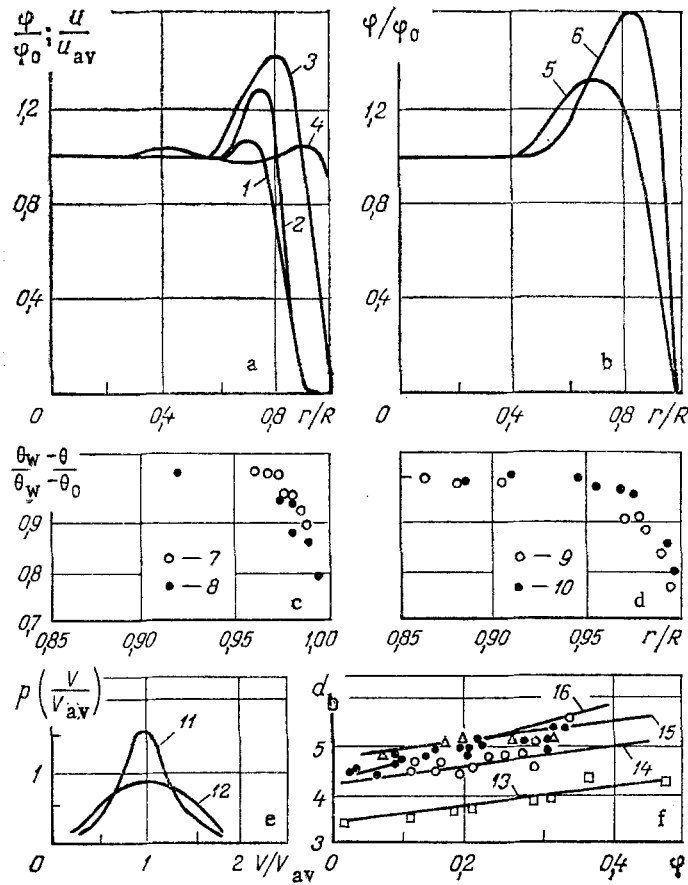


Fig. 2. Structure of descending bubble flows: a, c) concurrent flow; b, d, e) hovering of the gas phase; 1, 2, 4) peripheral entry; 1)  $u_{z_0} = 0.7$  m/sec,  $\varphi = 0.3$ ; 2)  $u_{z_0} = 0.7$  m/sec,  $\varphi = 0.06$ ; 3) central entry,  $u_{z_0} = 0.31$ ;  $\varphi = 0.17$ ; 4)  $u/u_{av}$ ,  $u_{z_0} = 0.7$  m/sec,  $\varphi = 0.15$ ; 5, 6) central entry,  $\theta = 4^\circ\text{C}$ ; 5)  $\varphi_{av} = 0.07$ ;  $u_{z_0} = 0.2$  m/sec; 6)  $\varphi_{av} = 0.29$ ,  $u_{z_0} = 0.12$  m/sec; 7)  $u_{z_0} = 0.4$  m/sec,  $\varphi_{av} = 0.064$ ; 8)  $u_{z_0} = 0.4$  m/sec,  $\varphi_{av} = 0.166$ ; 9)  $\varphi_{av} = 0.16$ ; 10) 0.22; 11) 0.14; 12) 0.39; 13-15) (unfilled points) concurrent flow,  $\theta = 4^\circ\text{C}$ ; 13)  $u_z = 0.575$  m/sec; 14) 0.345 m/sec; 15) 0.265 m/sec; 16) (filled points) hovering,  $\theta = 4-10^\circ\text{C}$ .  $d_b$ , mm.

for channels with peripheral entry of liquid and

$$B = 0,21Fr_{\sigma_0}^{0,52} (Ar_{\sigma_0}10^{-5})^{0,53} \quad (5)$$

for channels with central entry of liquid.

The amount of slippage  $C = u_g/u_z$  is a linear function of the flow-rate gas content.

When the liquid column is supplied in a descending film, a two-phase layer with a height of 100-500 mm develops in the immediate vicinity of the physical level. An analysis of the experimental results enabled us to generalize the gas content  $\varphi_h$  at the free level by the function

$$\varphi_h = A(L_{\sigma})B(K)(Fr_{\sigma_0}/Re_{l_0})10^4, \quad (6)$$

where

$$A(L_{\sigma}) = 0,185 + 0,012(L_{\sigma} \cdot 10^{-3}); \quad (7)$$

$$B(K) = 0,86 + 4,125 \cdot 10^{-2}(K/10^{14}). \quad (8)$$

When the liquid velocity reaches a certain critical value  $u_{z_0}^{cr}$ , there is a sharp increase in the column height of the two-phase layer:

$$u_{z_0}^{cr} / \left( \frac{g\sigma}{\rho_l - \rho_g} \right)^{0,25} = 18,6\varphi_h (1 - \varphi_h)^{5,7}. \quad (9)$$

In the hovering regime the height of the two-phase layer increases with an increase in the liquid velocity and decreases with an increase in temperature. Three characteristic sections can be distinguished in the distribution of gas content over the channel height. Formation of flow with hovering of the gas phase occurs in the first; the gas content is determined by the balance between the gas entering the layer from the gas cavity in the wall region with a descending liquid film and the gas returning to the gas cavity from the stream core. The section is characterized by large gradients of gas content. Farther away from the water level the conditions for hovering develop, when gas bubbles are in quasistatic equilibrium in the descending liquid flow. The second section is characterized by moderate gradients of gas content with an increase in pressure. As the pressure increases, the bubble sizes and the true liquid velocity decrease, the number of bubbles per unit volume of the stream changes, and all this leads to a change in the conditions of hovering. In the third section the gradient of gas content increases again and it decreases to zero. It is well known [3] that in the region of small bubble diameters the rise velocity decreases approximately linearly with a decrease in bubble diameter. Therefore, upon reaching a certain size with an increase in pressure, the bubbles will be carried out of the channel and their hovering will be impossible. And since bubbles of different sizes are present simultaneously in the stream and the group velocity of their rise varies in a more complicated way than the rise velocity of a single bubble, the decrease in gas content does not occur right in a certain cross section but over a certain length of the channel, and it is proposed to distinguish it as the third characteristic section of the two-phase layer.

The variation of gas content in the first two sections are approximated by the functions

$$\varphi = (\varphi_h - \varphi_0) \exp[-5(p/p_0 - 1)] + \varphi_0 (p_0/p)^n, \quad (10)$$

where

$$\varphi_0 = \varphi_h (0,88 - 0,04K \cdot 10^{-11}); \quad (11)$$

$$n = 1,5 + 0,2K \cdot 10^{-11}. \quad (12)$$

The boundary between the second and third sections is determined by the expression

$$\varphi_{cr} (1 - \varphi_{cr}) = (0,86 + 0,19L_\sigma \cdot 10^{-3})(23 + 1,6K \cdot 10^{-11}) u_{z_0} v_l / g d_\sigma^*, \quad (13)$$

while the variation of gas content in the third section is determined by the function

$$\varphi / \varphi_{cr} = 2 - (p/p_{cr})^m, \quad (14)$$

where

$$m = 5,45 (K \cdot 10^{-11})^{0,492}. \quad (15)$$

At nearly atmospheric pressure the gas content decreases with an increase in the liquid velocity (Fig. 1c) and approaches zero at  $u_{z_0} \sim 0,25$  m/sec, which corresponds to the rise velocity of a single bubble with a diameter of 3-4 mm. The dependence of the gas content on the velocity, like other characteristics of two-phase streams, proves to be different for central and peripheral entry of the liquid.

The hydraulic resistance was determined from the measured gradient of the static pressure and the true volumetric gas content:

$$\frac{1}{\rho_l g} \frac{\Delta p_{fr}}{\Delta x} = 1 - \varphi - \frac{1}{\rho_l g} \frac{\Delta p_w}{\Delta x}. \quad (16)$$

The hydraulic resistance in a two-phase stream, both concurrent and with hovering, is a strong function of the gas content (Fig. 1d, e). If the coefficient of hydraulic resistance is determined through the dynamic head of the liquid phase from the actual average velocity of the liquid (the error in determining  $C_f$  is 0.06) and, following Sato et al. [4], one assumes that the total frictional stress in the two-phase flow is composed of the frictional

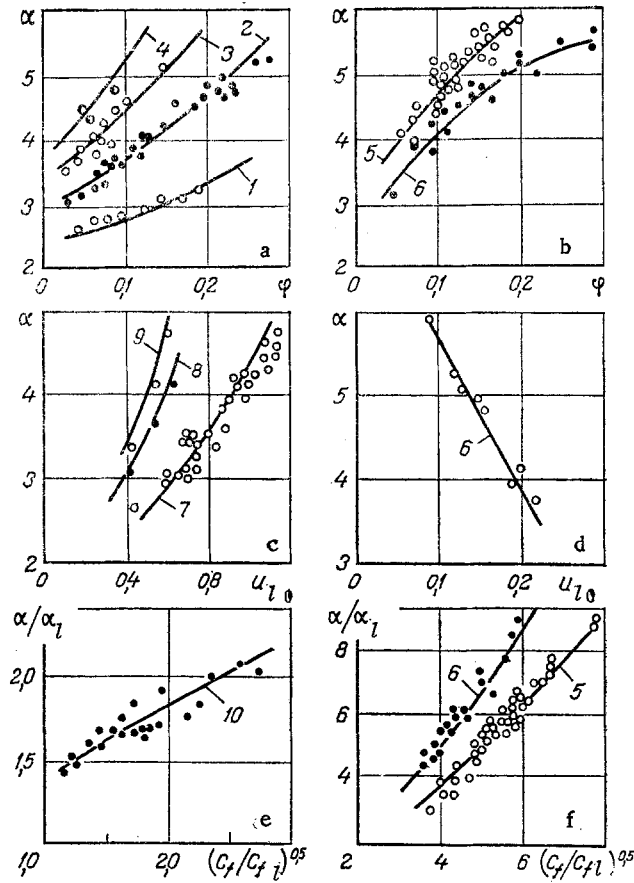


Fig. 3. Heat transfer to a descending bubble stream: a, c, e) concurrent flow; b, d, f) hovering of the gas phase; a)  $u_{z0} = 0.4-0.5$  m/sec; 1)  $\theta = 8^\circ\text{C}$ ; 2) 20; 3) 40; 4) 60; 5) 20; 6) 10; 7)  $\varphi = 0.01-0.06$ ,  $\theta = 5-10^\circ\text{C}$ ; 8)  $\varphi = 0.15$ ,  $\theta = 10^\circ\text{C}$ ; 9)  $\varphi = 0.25$ ,  $\theta = 10^\circ\text{C}$ ; 10)  $u_{z0} = 0.4-0.6$  m/sec,  $\theta = 10-60^\circ\text{C}$ .  $\alpha$ ,  $\text{kW/m}^2 \cdot ^\circ\text{K}$ ;  $u_{z0}$ , m/sec.

stress in the flow of the liquid phase alone and a correction for bubble mixing, then the total coefficient of friction can be represented in the form

$$C_f = C_{f1} + \Delta C_f. \quad (17)$$

The size of the correction  $\Delta C_f$  grows with an increase in the gas content, and for concurrent flow it comprises 40-90% of the total coefficient of friction (see Fig. 1d, e).

In the regime of hovering of the gas phase the losses to bubble mixing make the main contribution to the total hydraulic losses, reaching 90-98% (Fig. 1e).

The following function can be used to determine  $\Delta C_f$  in concurrent flow:

$$\Delta C_f = A_1(\varphi) u_0^n \left( \frac{p_{en}}{p} \right)^{-2.1} \left( \frac{M^2}{10^2} \right)^{-3.05} \left( \frac{\mu}{\mu_g} 10^{-2} \right)^{-1.4} d_0^{-0.6}. \quad (18)$$

For the case of the peripheral entry of the liquid-

$$A_1(\varphi) = (45\varphi^{0.65} + 1.5 \cdot 10^3 \varphi^{2.5}); \quad n = -2.185, \quad (19)$$

while for its central supply

$$A_1(\varphi) = (430\varphi^{1.825} + 12\varphi^{-0.05}); \quad n = -1.42. \quad (20)$$

The experimental data on  $\Delta C_f$  in the hovering regime are approximated by the following expressions:

peripheral entry

$$\Delta C_f = u_{\sigma}^{-1} [10 - 3,15 (K \cdot 10^{-11})^{-0,358}] [\varphi(1 - \varphi)]^{0,745}, \quad (21)$$

central entry

$$\Delta C_f = u_{\sigma}^{-1} [10 - 4,9 (K \cdot 10^{-11})^{-0,088}] [\varphi(1 - \varphi)]^{0,745}. \quad (22)$$

The results of the calculation of hydraulic resistance using the functions obtained are shown in Fig. 1d and e by solid lines.

The different values of the gas content and hydraulic resistance for peripheral and axial entry of the liquid, other conditions being equal, reflect the peculiarities of the internal structure of the flows. Characteristic results of investigations of the structure are shown in Fig. 2.

In both the concurrent flow (Fig. 2a) and the hovering regime (Fig. 2b) the distribution of gas content is characterized by the presence of a maximum at a certain distance from the wall and a large gradient in the wall region, where the gas content decreases to zero; in the core of the stream at  $r/R < 0.6$  the gas content remains practically constant. With peripheral entry of liquid a boundary layer of liquid in which gas is entirely absent is also retained at considerable distances from the entry (the data in Fig. 2a pertain to  $x/d = 100$ ). But with central entry of the liquid the gas content continuously approaches zero as one approaches the channel wall, while the maximum gas content lies at a distance equal to the average bubble diameter in the stream. The value of the maximum gas content increases with an increase in the average gas content in the stream and decreases with an increase in velocity. In the hovering regime (Fig. 2b) with the same average gas content the nonuniformity in the distribution of gas content over a cross section and its maximum values are higher than in a concurrent stream. This is connected with the fact that the liquid velocity is always lower for hovering than for concurrent flow.

The distribution of the liquid velocity (Fig. 2a) is also characterized by the presence of a maximum in the wall region and by large gradients near the wall, but the velocity maximum is less clearly expressed and its position is shifted toward the channel wall relative to the maximum of gas content. The liquid flow rate, found by integrating the velocity profile, practically coincides with a balanced profile (the departure is no more than 5%). The deformation of the distribution profile of the liquid velocity in comparison with one-phase flow is due to the turbulizing action of gas bubbles on the stream. The mixing influence of bubbles is also displayed in the distributions of the temperature of the mixture over a cross section. Both in concurrent flow (Fig. 3c) and with hovering (Fig. 2d) the temperature distribution is monotonic with a large gradient in the wall region. And the temperature remains constant at  $r/R < 0.95-0.97$ , i.e., over most of the channel cross section, while its entire change occurs in the narrow wall region at  $r/R > 0.95-0.97$ .

Bubbles with different volumes are present simultaneously in the flow. Their distribution is close to normal (Fig. 2e). The average equivalent bubble diameter in concurrent flow increases with an increase in gas content for a constant actual velocity and with a decrease in velocity for a constant gas content (Fig. 2f).

In the hovering regime the bubble diameter also increases with an increase in gas content, but in this case the liquid velocity decreases simultaneously (Fig. 1c). Therefore, in qualitative agreement with the data for concurrent flow, the increase in bubble diameter with an increase in gas content for hovering (Fig. 2f) takes place more intensely than in concurrent flow. The increase in pressure along the stream leads to a decrease in bubble diameter. The average bubble diameter hardly varies over a cross section of the channel.

As indicated above, the turbulizing action of gas bubbles on the stream leads to a considerable increase in hydraulic resistance in comparison with a one-phase stream (see Fig. 1d, e) and to intensification of heat transfer, and this was manifested in equalization of the temperature over a cross section of the channel (Fig. 2c, d).

Characteristic results from the investigation of the heat-transfer coefficient are presented in Fig. 3.

In both concurrent flow and hovering the heat-transfer coefficient increases with an increase in gas content and temperature (Fig. 3a, b). In concurrent flow the heat-transfer coefficient grows with an increase in the liquid velocity. But the opposite pattern is

observed for hovering: the heat-transfer intensity decreases with an increase in velocity. The reason for this is the simultaneous decrease in gas content (see Fig. 1c). Consequently, one can conclude that bubble mixing in the stream has a definite influence on the heat transfer.

A comparison of the data on hydraulic resistance and on heat transfer reveals their qualitative similarity. The retention of similarity in the transfer of heat and momentum in bubble gas—liquid streams was also pointed out in earlier work, such as [5].

The functions  $\alpha/\alpha_l = f[(C_f/C_{fl})^{0.5}]$  for concurrent flow and hovering are shown in Fig. 3e, f. In each case the function is nearly linear. The following functions can be recommended for finding the heat-transfer coefficients in descending bubble streams:

concurrent flow

$$\alpha/\alpha_l = P[1.05 + 0.385(C_f/C_{fl})^{0.5}], \quad (23)$$

$$P = 1.06 - 0.19 \cdot |7.5 - \text{Pr}_l|^{1.72},$$

hovering of the gas phase

$$\alpha/\alpha_l = [(C_f/C_{fl})^{0.5}]^n, \quad (24)$$

$$n = 0.585 + 0.0645 \text{Pr}_l.$$

The results of a calculation based on (23) and (24) are shown in Fig. 3 with solid lines.

#### NOTATION

$\alpha$ ,  $\alpha_l$ , coefficients of heat transfer to a two-phase stream and to a liquid;  $\beta$ , flow-rate volumetric gas content;  $\varphi$ , true volumetric gas content;  $\varphi_h$ , gas content below the water level in the hovering regime;  $\varphi_{cr}$ , gas content at the boundary between the second and third regions in the hovering regime;  $C_f$ ,  $C_{fl}$ , coefficients of frictional resistance in two-phase and one-phase flows;  $\Delta C_f$ , increase in the coefficient of friction due to bubble mixing;  $C$ , slippage coefficient;  $d_b$ , bubble diameter;  $d$ , channel diameter;  $R$ , channel radius;  $r$ , current radius;  $x$ , coordinate in the direction of motion of the stream;  $L$ , distance from the entrance to the water level in the channel;  $u$ , velocity;  $p$ ,  $p_{en}$ ,  $p_o$ , pressure in the cross section, at the entrance, and above the water level;  $\rho$ , density;  $\theta$ ,  $\theta_w$ ,  $\theta_m$ , temperature, temperature at the wall, and at the channel axis;  $\nu$ , kinematic viscosity;  $\sigma$ , coefficient of surface tension at the liquid—gas interface;  $V$ ,  $V_{av}$ , volume of a bubble and average volume of a bubble;  $\text{Pr}_l$ , Prandtl number of the liquid;  $\text{Ar}_\sigma = g[\sigma/g(\rho_l - \rho_g)]^{3/2}/\nu_l^2$ ;  $d_\sigma^* = [\sigma/g(\rho_l - \rho_g)]^{0.5}$ ;  $\text{Fr}_{\sigma o} = u^2 \nu_o / g d_\sigma^*$ ;  $d_\sigma = d/d_\sigma^*$ ;  $L_\sigma = L/d_\sigma^*$ ;  $M^2 = g \rho_l d_\sigma^* / p_{en}$ ;  $u_\sigma = u_l / [\sigma/g(\rho_l - \rho_g)]^{0.25}$ ;  $\text{Re}_{\nu o} = u_l d / \nu_l$ ;  $K = \sigma^3 / g \rho_l^3 \nu_l^4$ .

#### LITERATURE CITED

1. M. Kh. Ibragimov, V. P. Bobkov, and N. A. Tychinskii, "Behavior of the gas phase in a turbulent stream of a water—gas mixture in a channel," *Teplofiz. Vys. Temp.*, 11, No. 5, 1051-1061 (1973).
2. B. G. Ganchev, V. G. Peresad'ko, and V. I. Vasilenko, "Determination of the volume of bubbles in a two-phase stream by the method of continuous sampling," in: *Hydraulics. Modern Problems of Hydrodynamics and Heat Exchange in Elements of Power Plants and Cryogenic Technology* [in Russian], VZMI, Moscow (1978), pp. 21-31.
3. S. S. Kutateladze and M. A. Styrikovich, *Hydrodynamics of Gas—Liquid Systems* [in Russian], Énergiya, Moscow (1976).
4. Y. Sato, M. Sadatomi, and K. Sekoguchi, "Momentum and heat transfer in two-phase bubble flow, Parts I and II," *J. Multiphase Flow*, 7, No. 2, 167-177, 179-190 (1981).
5. V. N. Sokolov and I. V. Domanskii, *Gas—Liquid Reaction Vessels* [in Russian], Mashinostroenie, Leningrad (1976).